Simultaneous dual gas QEPAS sensing of water and methane/nitrous oxide

A. Sampaolo[1], P. Patimisco[1], M. Giglio[1], G. Menduni[1,2], A. Elefante[1], V. Passaro[2], F.K. Tittel[3], and V. Spagnolo[1]

[1] PolySense Lab - Dipartimento Interateneo di Fisica, Politecnico and University of Bari, Via Amendola 173, Bari, Italy;
[2] Photonics Research Group, Dipartimento di Ingegneria Elettrica e dell'informazione, Politecnico di Bari, Via Orabona 4, Bari, 70126, Italy;
[3]Electrical and Computer Engineering Department, Rice University, 6100 Main St., Houston TX, 77005 USA;

ABSTRACT

Simultaneous detection of different trace gases is an important topic in many applications, such as breath analysis, environmental monitoring and oil exploration. Quartz-enhanced photoacoustic spectroscopy offers a good solution of this problem, due to the possibility to operate the quartz resonators at the fundamental and overtone resonance frequencies by simultaneously exciting two different antinodes with two different laser sources. In this work we employed a custom spectrophone coupled with a diode laser and a quantum cascade laser for simultaneous detection of water vapor and methane/nitrous oxide with minimum detection limits in the ppb range.

Keywords: quartz-enhanced photoacoustic spectroscopy, dual gas detection, overtone vibration mode, methane, nitrous oxide

1. INTRODUCTION

Simultaneous detection and quantification of different components in a gas mixture is usually required in several applications, such as in the detection of isotopes concentration ratios or human breath analysis for monitoring different biomarkers at the same time. For optical gas sensing techniques, multi-gas detection is performed by probing multiple transitions belonging to different gas species. The conventional approach is to use a single light source having wide spectral coverage, such as a widely tunable monolithic diode laser [1] or an external cavity laser [2-5]. Multi-gas detection is achieved by scanning the laser current in all its dynamic range or alternatively by switching the laser current (and thus the laser wavelength) among values corresponding to absorption peaks of different gas species. In this case, the detection of multiple species is not really simultaneous because of the time needed to switch the laser current between different values. Hence, the only approach for a real simultaneous detection of different gas species is to multiplex several independently operated laser sources (one per each selected gas species) in combination with a single detector, by employing a frequency-modulated multiplexing scheme [6]. This detection scheme cannot be applied to gas sensing spectroscopic techniques based on multi-pass cells or high finesse optical cavities mainly due to the complexity of the apparatus [7]. Photoacoustic spectroscopy has proved to be a reliable technique for trace gas detection, allowing real time and in situ measurements of gas concentration with high sensitivity and selectivity [8]. Quartz-enhanced photoacoustic spectroscopy (QEPAS) uses a quartz tuning fork (QTF) to detect weak sound waves generated by the gas when this latter absorbs modulated laser light [9-11]. The laser light is focused between QTF prongs, close to the antinode point of the resonance mode of the vibrating prong. Then, the laser light is modulated at the resonance frequency (or one of its subharmonics) of one of QTF in-plane vibrational modes [12-15]. The resonance frequency of flexural modes strongly depends on the geometry of the prong and cannot exceed 40 kHz. This constraint is imposed by non-radiative relaxation times (typically of few microseconds) needed for efficient sound wave generation in the absorbing gas [16-18]. When the fundamental flexural mode has a resonance frequency < 4 kHz, the first overtone mode (about 6.2 times higher than the frequency of the fundamental mode) becomes also accessible for QEPAS operation. The

Quantum Sensing and Nano Electronics and Photonics XVI, edited by Manijeh Razeghi, Jay S. Lewis, Eric Tournié, Giti A. Khodaparast, Proc. of SPIE Vol. 10926, 109262L

first overtone mode has two distinct antinodes, one on the top of the prong (coincident with the single antinode point of the fundamental mode) and the other one close to the middle of the prong [19-28]. This opens the way to the possibility of exciting the QTF at the fundamental and at the first overtone resonance modes simultaneously by focusing one laser source close to the top of the prong (to excite the fundamental mode) and a second laser source close to the middle of the prong (to excite the first overtone mode) [6]. In this way, a frequency-modulated multiplexing scheme with two laser sources for simultaneous dual-gas detection can be realized by using the QEPAS technique.

In this work we report on a simultaneous dual-gas QEPAS sensor acoustically equipped with two pairs of micro-resonator dual-tube systems, operating i) in the mid-infrared spectral range at 7730 nm for methane and nitrous oxide detection, by means of a quantum cascade laser and ii) in the near-infrared range at 1392 nm for water vapor monitoring by employing a diode laser.

2. ACOUSTIC DETECTION MODULE ARCHITECTURE

The QTF employed in this work for simultaneous dual-gas detection has prong lengths of 17 mm, a thickness of 1 mm and a quartz crystal width of 0.25 mm. The spacing between the two prongs is 0.7 mm. The fundamental mode has a resonance frequency of f_0 = 2871.5 Hz and a quality factor of 6680, measured at an air pressure of 200 Torr. At the same pressure, the first overtone mode has a resonance frequency of f_1= 17747.7 Hz and a quality factor of 17070 [29]. The two antinode points for the first overtone mode lie at the top of the QTF (as for the fundamental mode) and 9 mm far from the top of the prongs [26]. To enhance the QEPAS signal, the QTF is usually acoustically coupled with a pair of micro-resonator tubes positioned on both sides of the QTF and acting as sound amplifiers. Since the fundamental and first overtone mode have to be excited simultaneously, two pairs of micro-resonator tubes are needed, one located close to the top of the prong (to enhance the fundamental mode) and the other one 9 mm far from the top of the prong (to enhance the first overtone mode). A sketch of the QTF with two pairs of micro-resonator tubes, usually referred as the QEPAS spectrophone, is shown in Fig. 1.

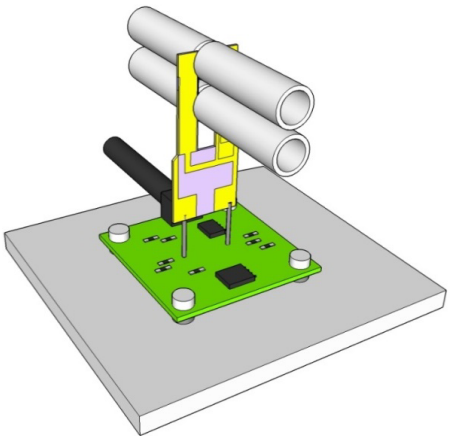

Figure 1. Schematic of the spectrophone implemented in this work. The spectrophone is composed of a QTF and two dual-tube micro-resonators aligned perpendicular to the QTF plane; one pair of tubes is positioned close to the top of the QTF (where the antinode point of the fundamental mode lies) and the other one is located 9 mm below the top of the prongs (where is located the second antinode point of the QTF first overtone mode).

The geometrical parameters influencing the sensor performance are the internal diameter and the length of the two tubes together with the spacing between the tube and the surface of the QTF [10, 30]. The optimal length l of the tubes depends on the interaction of two resonator tubes and their acoustic coupling to the QTF. Experimental studies showed that the tube length has to fall between $\lambda_s/4$ and $\lambda_s/2$, where $\lambda_s=v/f$ is the sound wavelength, v is the speed of the sound (343 m/s in air) and f is the frequency of the sound wave [10]. For the first overtone mode (λ_s = 19.3 mm), 4.8 < l < 9.6 mm, and l = 8.5 mm was selected. For the fundamental mode (λ_s = 119.4 mm), the optimal length should be between 30 mm and 60 mm. This range of tube lengths is unpractical for optical alignment. For this reason, tubes 9.5 mm-long, comparable with those used for the first overtone mode were employed for the fundamental mode, practical for the overall size of the spectrophone. The choice of the optimal tube internal diameter (ID) can be related to the QTF prongs spacing. When the

tube diameter is larger than the prongs spacing, the gap between two tubes becomes less important and the tubes are acoustically coupled with the QTF. When the tube diameter becomes comparable with the prongs spacing, the acoustic coupling is reduced [10]. Experimental studies showed that the optimal ID should be ~1.5 times the prong spacing, which means an ID = 1.36 mm for both pairs of tubes. The gaps size between the QTF and the tubes was fixed to 150 μm.

3. SENSOR ARCHITECTURE

The spectrophone was mounted in a QEPAS sensor system depicted in Fig. 2.

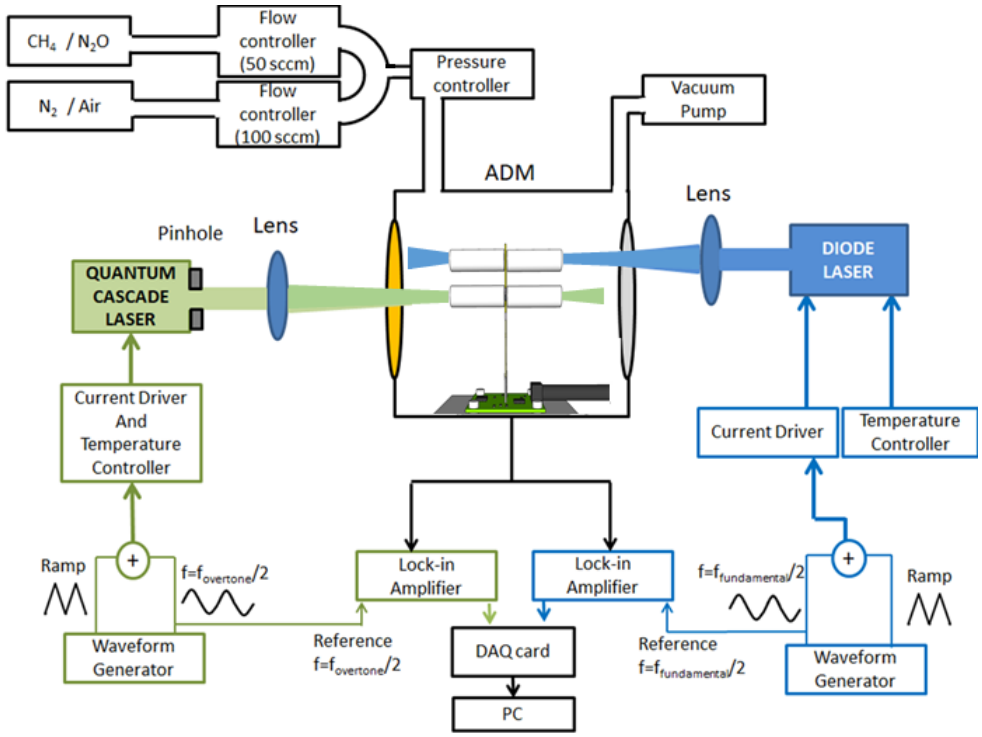

Figure 2. Schematic of the dual gas QEPAS sensor system.

Two lasers were used as QEPAS excitation sources. A diode laser emitting at 1.39 μm was used to excite the fundamental flexural mode of the QTF and to target water vapor. A quantum cascade laser (QCL) emitting at 7.73 μm was used to excite the first overtone mode and to target CH_4/N_2O. The spectrophone was enclosed in a gas cell equipped on one side with a CaF_2 window to transmit the laser diode light and on the other side with an AR-coated ZnSe window to transmit the QCL light. The diode laser beam was focused between the QTF prongs and through the tubes located close to the antinode point of the fundamental mode by means of an AR-coated N-BK7 lens with a focal length 75 mm. The QCL beam was spatially filtered by using a pinhole and then focused through the tubes located at the second antinode point of the first overtone mode, by means of an AR-coated ZnSe lens having a focal length 75 mm. The QTF piezoelectric current is converted into a voltage signal by using a trans-impedance preamplifier and then sent to two lock-in amplifiers. A wavelength modulation technique with *2f*-detection was implemented to detect the QEPAS signal [31-32]: a sinusoidal modulation was applied to the diode laser current and to the quantum cascade laser current at $f_0/2$ and $f_1/2$, respectively. The QTF response was simultaneously demodulated at f_0 and f_1 by using two lock-in amplifiers. QEPAS spectral measurements were performed by linearly varying both the diode and QCL current. Two waveform generators were used for driving both QCL and diode current driver, simultaneously. The gas line consists of 3 cylinders, two gas flow controllers, a pressure controller and a vacuum pump. The cylinders contain: 1000 ppm certified concentration of CH_4 in N_2, 10000 ppm certified concentration of N_2O in N_2 and pure N_2 (acting as diluting gas for mixtures realized starting from certified concentrations). Cylinders with CH_4 and N_2O mixtures were used alternatively

to target one or the other gas. The mixture flow rate (and thus the gas target concentration in diluted mixtures) was set by using a LabVIEW-based software. The pressure controller and vacuum pump were used to maintain the pressure of the gas flowing through the spectrophone at a fixed value of 200 Torr.

4. SENSOR PRELIMINARY STUDY

A preliminary study was performed to study the QTF response when the fundamental and first overtone mode are simultaneously excited. Both laser sources were tuned to detect two water vapor absorption lines located at 7181.16 cm^{-1} (linestrength of $1.4 \cdot 10^{-20}$ cm/mol) and at 1297.18 cm^{-1} (with a linestrength of $4 \cdot 10^{-22}$ cm/mol) for the laser diode and QCL, respectively [33]. The pressure of the gas was set to 200 Torr. Figure 3(a) shows the QTF signal demodulated at f_0 when only the fundamental mode is excited (blue circles) and when the two lasers simultaneously excite the fundamental and first overtone modes of the QTF (red squares). The overlap of the two curves indicates that when the QTF oscillates in the fundamental mode, the simultaneous excitation of the 1st overtone mode does not affect the fundamental QEPAS signal, i.e., the fundamental flexural mode is independent of the 1st overtone flexural mode. Similarly, Figure 3(b) shows the QTF signal demodulated at f_1 when only the overtone mode is excited (blue circles) and when both the QTF vibrational modes are excited (red squares). Hence, when the QTF operates in the 1st overtone flexural mode, no interference effects are observed if the QTF fundamental mode is also excited. Therefore, both the fundamental and 1st overtone QTF signals can be separately extracted when both modes are simultaneously excited.

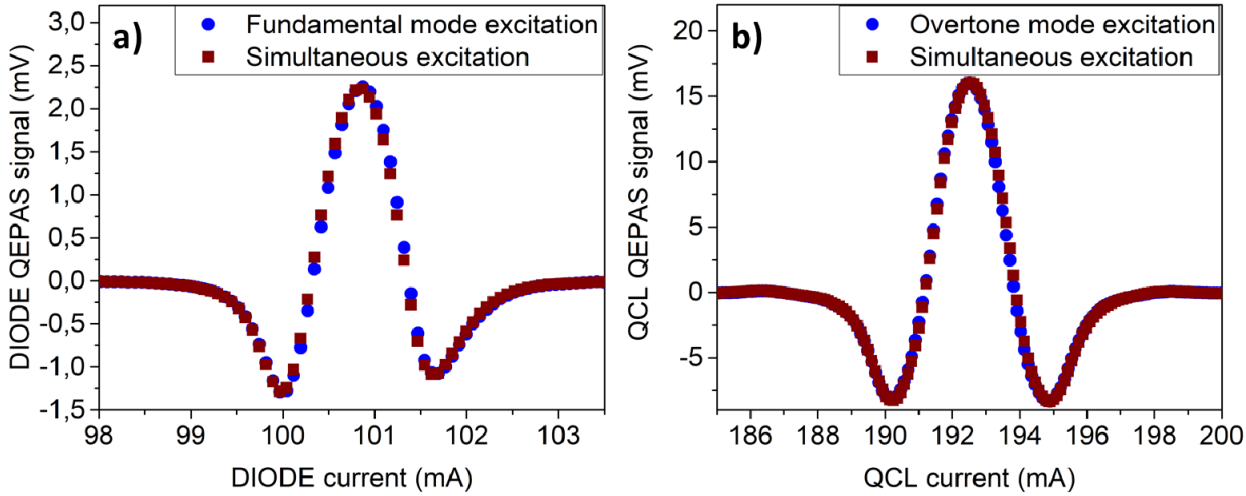

Figure 3. (a) QEPAS spectral scans of the water absorption line located at 7181.16 cm^{-1} measured by the detection channel of the QTF fundamental mode, when only the fundamental mode is excited (blue circles) and both the fundamental and first overtone modes are excited (red squares). (b) QEPAS spectral scan of the absorption line of water vapor at 1297.18 cm^{-1} detected by the detection channel of the QTF first overtone mode, when only the first overtone mode is excited (blue circles) and both the fundamental and first overtone modes are excited (red squares).

For the water absorption line detected using the laser diode, a peak signal of V_{peak}= 2.26 mV with a 1σ noise level of $1\sigma_{noise}$= 0.9 μV was measured when the QTF was excited only at the fundamental mode, comparable with the values V_{peak}= 2.23 mV and $1\sigma_{noise}$= 1.2 μV obtained when both the QTF modes were excited. For the water vapor detected using the QCL, a V_{peak}= 16.03 mV with $1\sigma_{noise}$= 132 μV was obtained when only the first overtone is excited, comparable with V_{peak}= 16.03 mV with $1\sigma_{noise}$= 138 μV obtained for the simultaneous excitation of both vibrational modes.

5. SENSOR CALIBRATION

Once demonstrated that there is no cross-talk between two QTF vibrational modes, the first overtone mode was excited to detect CH_4 or N_2O, and the fundamental QTF vibrational mode to monitor water vapor in the gas mixture, simultaneously. The selected CH_4 absorption line is peaked at 1297.47 cm^{-1} with a linestrength of $3.9 \cdot 10^{-20}$ cm/mol and the N_2O absorption line is located at 1297.05 cm^{-1} with a linestrength of 1.7 10^{-19} cm/mol [33]. The pressure of the gas

was set to 200 Torr with a flow of 30 sccm. The QCL temperature was set to 12.5 °C and the laser amplitude modulation providing the highest QEPAS signal resulted 35mV for the CH_4 absorption line and 130 mV for the N_2O line. For the sensor validation, different CH_4 concentrations in the 50–750 ppm range were realized by diluting the calibrated mixture of 1000 ppm CH_4:N_2 in dry N_2. Similarly, different N_2O concentrations in the 300–800 ppm range were generated by diluting the calibrated mixture of 10000 ppm N_2O:N_2 in dry N_2. For each spectral scan, the peak value was extracted and plotted as a function of the gas target concentration in the mixture, both for CH_4 and N_2O. Figure 4 shows the calibration curves (blue squares) and the best linear fit (red solid line) obtained for CH_4 (Fig. 4(a)) and N_2O (Fig. 4(b)).

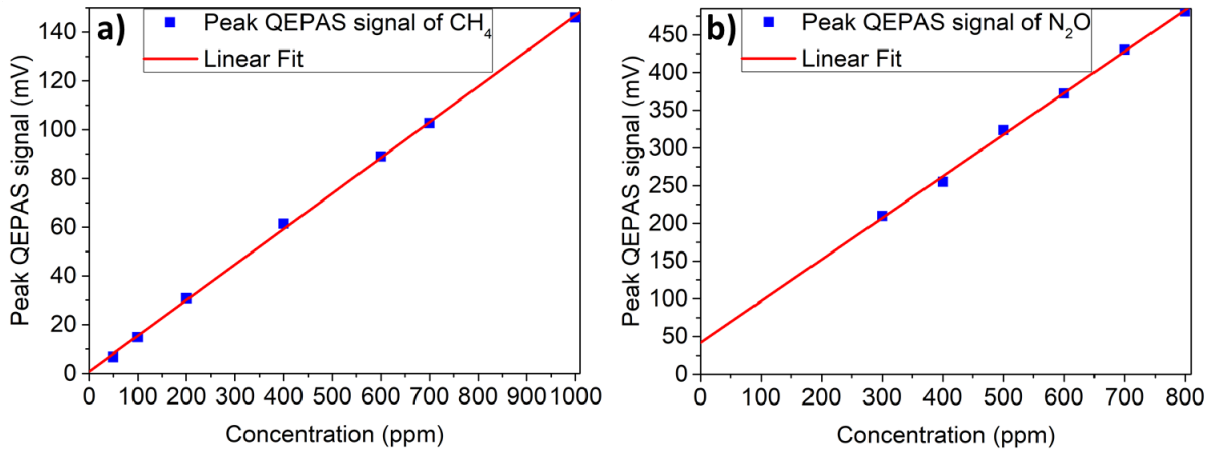

Figure 4. (a) QEPAS peak signal (blue squares) as a function of the CH_4 concentration. The red solid line is the best linear fit of the experimental data. The R-squared value is R = 0.999. (b) QEPAS peak signal (blue squares) as a function of the N_2O concentration. The red solid line is the best linear fit of the experimental data. The R-squared value is R = 0.998. Both calibration curves were obtained at a gas pressure of 200 Torr.

The results clearly showed the linearity of the QEPAS signal as a function of the gas concentration, both for CH_4 (with a slope of 0.15 mV/ppm) and N_2O (slope of 0.55 mV/ppm) detection.

6. DUAL GAS QEPAS SENSOR PERFORMANCE

The QEPAS sensor was used to detect CH_4 or N_2O using the QCL modulated to excite the first QTF overtone mode, while the laser diode is modulated to excite the fundamental mode of the QTF in order to monitor the water vapor concentration in the gas mixture. To add water vapor in the gas mixture, the calibrated mixture of 1000 ppm CH_4:N_2 was diluted by using wet air. The temperature of the laser diode was set to 25°C and the laser current was scanned from 50 to 115 mA using a slow voltage ramp with frequency of 2 mHz applied to the laser current driver. The optimal laser diode modulation amplitude maximizing the QEPAS signal was 12 mV. The temperature of the QCL was set to 12.5°C and the laser current was scanned from 145 to 280 mA applying a ramp of 2 mHz to the QCL current driver. The QCL current was modulated with a sinusoidal waveform with a peak-to-peak amplitude of 35 mV. In Fig.5 (a) the QEPAS scan obtained by demodulating the QTF signal at f_1 is shown. The largest peak signal of V_{peak} = 61.4 mV occurring at a QCL current I_{QCL}= 243.7 mA is due to the selected CH_4 absorption line; other small features peaked at I_{QCL} = 161.9 mA, 185.6 mA, 224.8 mA and 231.8 mA are due to other CH_4 absorption lines with weaker linestrengths, while the absorption feature peaked at I_{QCL} = 263.7 mA is due to a water vapor line, as confirmed by using the HITRAN database [33]. In Fig.5(b) the QEPAS scan demodulated at f_0 is reported. The selected water vapor absorption line corresponds to a diode current of I_D =100.15 mA. The other water vapor absorption lines are peaked at I_D = 79.3 mA, 88.5 mA, 108.27 mA.

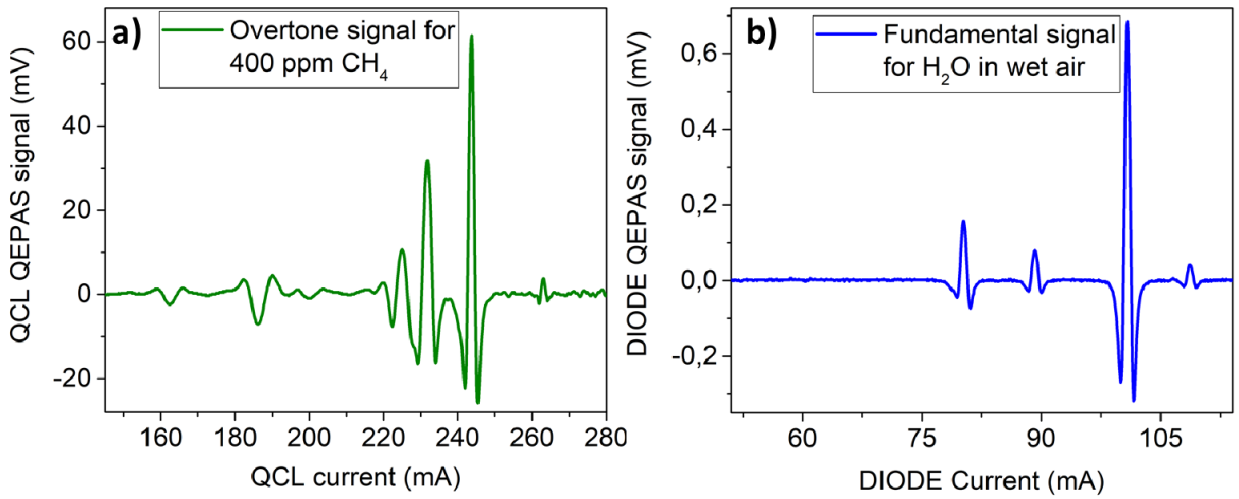

Figure 5. Simultaneous QEPAS spectral scans for a mixture of 400 ppm of CH_4 in wet air, at 200 Torr (a) CH_4 signal detected exciting the QTF at the first overtone mode using the QCL (b) Water vapor signal detected exciting the QTF at the fundamental mode using the diode laser.

For the simultaneous detection of N_2O and water vapor, the laser diode settings were unchanged. The QCL temperature was fixed at 12.5°C and the laser current was modulated with a sinusoidal waveform with a peak-to-peak amplitude of 130 mV, while it is linearly scanned from 150 mA to 290 mA at a frequency of 2 mHz. The obtained spectral scans are shown in Figure 6.

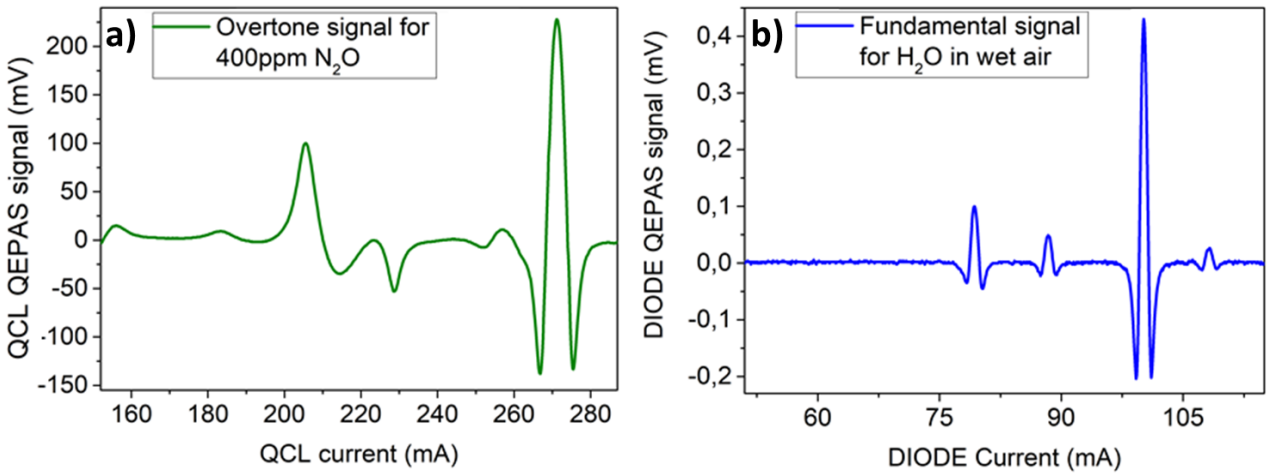

Figure 6. Simultaneous QEPAS spectral scans for a mixture of 400 ppm of N_2O in wet air at 200 Torr (a) N_2O signal detected exciting the QTF at the first overtone mode using the QCL (b) Water vapor signal detected exciting the QTF at the fundamental mode using the diode laser.

The selected N_2O absorption line corresponds to a QCL current of 271.1 mA and reaches a peak value of V_{peak} = 227 mV in Fig.6 (a). The absorption feature peaked at 217.5 mA is due to a weaker N_2O absorption line. From an estimation of the signal-to-noise ratio, with an integration time of 100 ms a minimum detection limit (MDL) of 18 ppb was reached for methane, which is 5 times better with respect to the one measured in our previous work reported in ref [34]. A minimum detection limit of 4.5 ppb was achieved for the N_2O at the same integration time.

7. CONCLUSIONS

In this work, we realized a dual-gas QEPAS sensor for the simultaneous detection of CH_4/H_2O and N_2O/H_2O. A laser diode and a quantum cascade laser were used to excite both the fundamental and the first overtone mode of a custom-made quartz tuning fork, respectively. We demonstrated that there is no interference effect between the two vibrational modes of the QTF. The QEPAS sensor was tested both for the simultaneous detection of H_2O and CH_4 reaching a MDL of 18 ppb for methane detection, and for the simultaneous detection of H_2O and N_2O, reaching a MDL of 4.5 ppb for N_2O.

AKNOWLEDGMENTS

The authors from Dipartimento Interateneo di Fisica di Bari acknowledge financial support from THORLABS GmbH, within the joint research laboratory PolySense. Frank K. Tittel acknowledges support by the Welch Foundation under Grant No. C0568.

REFERENCES

[1] Giglio, M., Patimisco, P., Sampaolo, A., Zifarelli, A., Blanchard, R., Pfluegl, C., Witinski, M.F., Vakhshoori, D., Tittel, F.K., and Spagnolo, V., Nitrous oxide quartz-enhanced photoacoustic detection employing a broadband distributed-feedback quantum cascade laser array," Appl. Phys. Lett. 113, 171101 (2018).

[2] Patimisco, P., Spagnolo, V., Vitiello, M. S., Tredicucci, A., Scamarcio, G., Bledt, C. M., and Harrington, J. A., "Coupling external cavity mid-IR quantum cascade lasers with low loss hollow metallic/dielectric waveguides," Appl. Phys. B 108, 255–260 (2012).

[3] Sampaolo, A., Patimisco, P., Giglio, M., Chieco, L., Scamarcio, G., Tittel, F.K., and Spagnolo, V., "Highly sensitive gas leak detector based on a quartz-enhanced photoacoustic SF_6 sensor," Opt. Express 24, 15872-15881 (2016).

[4] Siciliani de Cumis, M., Viciani, S., Borri, S., Patimisco, P., Sampaolo, A., Scamarcio, G., De Natale, P., D'Amato, F., and Spagnolo, V., "Widely tunable mid-infared fiber coupled quartz-enhanced photoacoustic sensor for enviromental monitoring," Opt. Express 22, 28222-28231 (2014).

[5] Spagnolo, V., Patimisco, P., Borri, S., Scamarcio, G., Bernacki, B.E., and Kriesel, J., "Mid-infrared fiber-coupled QCL-QEPAS sensor," Appl. Phys. B 122, 25-33 (2013).

[6] Wu, H., Yin, X., Dong, L., Pei, K., Sampaolo, A., Patimisco, P., Zheng, H., Ma, W., Zhang, L., Yin, W., Xiao, L., Spagnolo, V., Jia, S., Tittel, F.K., "Simultaneous dual-gas QEPAS detection based on a fundamental and overtone combined vibration of quartz tuning fork," Appl. Phys. Lett. 110, 121104 (2017).

[7] Hodgkinson, J., and Tatam, R.P., "Optical gas sensing: A review," Meas. Sci. Technol., 24, 012004:1–012004:59, 2013.

[8] Elia, A., Lugarà, P.M., di Franco, C., Spagnolo, V., "Photoacoustic Techniques for Trace Gas Sensing Based on Semiconductor Laser Sources," Sensors 9, 9616–9628 (2009).

[9] Patimisco, P., Scamarcio, G., Tittel, F.K., Spagnolo, V., "Quartz-Enhanced Photoacoustic Spectroscopy: A Review," Sensors 14, 6165-6206 (2014).

[10] Patimisco, P., Sampaolo, A., Zheng, H., Dong, L., Tittel, F.K. and Spagnolo V., "Quartz enhanced photoacoustic spectrophones exploiting custom tuning forks: a review," Adv. Phys. X 2, 169-187 (2016).

[11] Patimisco, P., Sampaolo, A., Dong, L., Tittel, F.K., Spagnolo V., "Recent advances in quartz enhanced photoacoustic sensing," Appl. Phys. Rev., 011106 (2018).

[12] Jahjah, M., Jiang, W., Sanchez, N.P., Ren, W., Patimisco, P., Spagnolo, V., Herndon, S.C., Griffin, R.J., and Tittel, F.K., "Atmospheric CH_4 and N_2O measurements near Greater Houston area landfills using QCL-based QEPAS sensor system during DISCOVERY-AQ 2013," Opt. Lett. 39, 957-960 (2014).

[13] Viciani, S., Siciliani de Cumis, M., Borri, S., Patimisco, P., Sampaolo, A., Scamarcio, G., De Natale, P., D'Amato, F., and Spagnolo, V., "A quartz-enhanced photoacoustic sensor for H_2S trace-gas detection at 2.6 μm," Appl. Phys. B 119, 21-27 (2014).

[14] Giglio, M., Patimisco, P., Sampaolo, A., Scamarcio, G., Tittel, F. K., and Spagnolo, V., "Allan Deviation Plot as a Tool for Quartz-Enhanced Photoacoustic Sensors Noise Analysis," IEEE Trans. Ultrason. Ferroelect. Freq. Control, 63, 555-560 (2016).

[15] Zheng, H., Dong, L., Sampaolo, A., Wu, H., Patimisco, P., Yin, X., Ma, W., Zhang, L., Yin, W., Spagnolo, V., Jia, S., Tittel, F.K., "Single-tube on-beam quartz-enhanced photoacoustic spectroscopy," Opt. Lett. 41, 978-981 (2016).
[16] Wysocki, G., Kosterev, A.A., and Tittel, F.K., "Influence of molecular relaxation dynamics on quartz-enhanced photoacoustic detection of CO_2 at $\lambda = 2$ μm," Appl. Phys. B 85, 301-306 (2006).
[17] Kosterev, A.A., Mosely, T.S., and Tittel, F.K., "Impact of humidity on quartz-enhanced photoacoustic spectroscopy based detection of HCN," Appl. Phys. B 85, 295–300 (2006).
[18] Ren, W., Jiang, W., Sanchez, N.P., Patimisco, P., Spagnolo, V., Zah, C., Xie, F., Hughes, L.C., Griffin, R.J., and Tittel, F.K., "Hydrogen peroxide detection with quartz-enhanced photoacoustic spectroscopy using a distributed-feedback quantum cascade laser," Appl. Phys. Lett. 104, 041117 (2014).
[19] Wang, Q., Wang, Z., Ren, W., Patimisco, P., Sampaolo, A., and Spagnolo, V., "Fiber-ring laser intracavity QEPAS gas sensor using a 7.2 kHz quartz tuning fork," Sensor Actuat. B-Chem. 227268, 512-518 (2018).
[20] Wu, H., Sampaolo, A., Dong, L., Patimisco, P., Liu, X., Zheng, H., Yin, X., Ma, W., Zhang, L., Yin, W., Spagnolo, V., Jia, S., and Tittel, F.K., "Quartz enhanced photoacoustic H_2S gas sensor based on a fiber-amplifier source and a custom tuning fork with large prong spacing," Appl. Phys. Lett. 107, 111104 (2015).
[21] Sampaolo, A., Patimisco, P., Giglio, M., Vitiello, M.S., Beere, H.E., Ritchie. D.A., Scamarcio, G., Tittel, F. K., and Spagnolo, V., "Improved Tuning Fork for Terahertz Quartz-Enhanced Photoacoustic Spectroscopy," Sensors, 16, 439 (2016).
[22] Spagnolo, V., Patimisco, P., Pennetta, R., Sampaolo, A., Scamarcio, G., Vitiello, M.S., Tittel, F.K., "THz Quartz-enhanced photoacoustic sensor for H_2S trace gas detection," Opt. Express 23, 7574-7582 (2015).
[23] Sampaolo, A., Patimisco, P., Dong, L., Geras, A., Scamarcio, G., Starecki, T., Tittel, F. K., and Spagnolo, V., "Quartz-enhanced photoacoustic spectroscopy exploiting tuning fork overtone modes," Appl. Phys. Lett. 107, 231102 (2015).
[24] Zheng, H., Dong, L., Patimisco, P., Wu, H., Sampaolo, A., Yin, X., Li, S., Ma, W., Zhang, L., Yin, W., Xiao, L., Spagnolo, V., Jia, S., Tittel, F.K., "Double antinode excited quartz-enhanced photoacoustic spectrophone," Appl. Phys. Lett. 110, 021110 (2017).
[25] Zheng, H., Dong, L., Sampaolo, A., Wu, H., Patimisco, P., Ma, W., Zhang, L., Yin, W., Xiao, L., Spagnolo, V., Jia, S., and Tittel, F.K., "Overtone resonance enhanced single-tube on-beam quartz enhanced photoacoustic spectrophone," Appl. Phys. Lett. 109, 111103 (2016).
[26] Tittel, F.K., Sampaolo, A., Patimisco, P., Dong, L., Geras, A., Starecki, T., and Spagnolo, V., "Analysis of overtone flexural modes operation in quartz-enhanced photoacoustic spectroscopy," Opt. Express 24, A682-A692 (2016).
[27] Patimisco, P., Sampaolo, A., Dong, L., Giglio, M., Scamarcio, G., Tittel, F.K., and Spagnolo, V., "Analysis of the electro-elastic properties of custom quartz tuning forks for optoacoustic gas sensing," Sensor Actuat. B-Chem. 227, 539-546 (2016).
[28] Patimisco, P., Borri, S., Sampaolo, A., Beere, H.E., Ritchie, D.A., Vitiello, M.S., Scamarcio, G., and Spagnolo, V., "Quartz enhanced photo-acoustic gas sensor based on custom tuning fork and terahertz quantum cascade laser," Analyst 139, 2079-2087 (2014).
[29] Patimisco, P., Sampaolo, A., Mackowiak, V., Rossmadl, H., Cable, A., Tittel, F.K., and Spagnolo, V., "Loss Mechanisms Determining the Quality Factors in Quartz Tuning Forks Vibrating at the Fundamental and First Overtone Modes," IEEE Trans. Ultrason. Ferroelect. Freq. Control 65, 1951-1957 (2018).
[30] Dong, L., Kosterev, A.A., Thomazy, D., Tittel, F.K., "QEPAS spectrophones: design, optimization, and performance," Appl. Phys. B 100, 627–635 (2010).
[31] Bidaux, Y., Bismuto, A., Patimisco, P., Sampaolo, A., Gresch, T., Strubi, G., Blaser, S., Tittel, F.K., Spagnolo, V., Muller, A., and Faist, J., "Mid infrared quantum cascade laser operating in pure amplitude modulation for background-free trace gas spectroscopy," Opt. Express 24, 26464-26471 (2016).
[32] Patimisco, P., Sampaolo, A., Bidaux, Y., Bismuto, A., Schott, M., Jiang, J., Muller, A., Faist, J., Tittel, F.K., and Spagnolo, V., "Purely wavelength- and amplitude-modulated quartz-enhanced photoacoustic spectroscopy," Opt. Express 24, 25943-25954 (2016).
[33] https://hitran.org/
[34] Sampaolo, A., Csutak, S., Patimisco, P., Giglio, M., Menduni, G., Passaro, V., Tittel, F.K., Deffenbaugh, M., and Spagnolo, V. "Methane, ethane and propane detection using a compact quartz enhanced photoacoustic sensor and a single interband cascade laser". Sensors and Actuators B: Chemical (2018).